Conformation of a Pentacosapeptide Representing the RNA-Binding N-Terminus of Cowpea Chlorotic Mottle Virus Coat Protein in the Presence of Oligophosphates: A Two-Dimensional Proton Nuclear Magnetic Resonance and Distance Geometry Study

Marinette van der Graaf,[‡,§] Ruud M. Scheek,[∥] Catharina C. van der Linden,[‡,⊥] and Marcus A. Hemminga*[,‡]

Department of Molecular Physics, Agricultural University, Dreijenlaan 3, 6703 HA Wageningen, The Netherlands, and BIOSON Research Institute, University of Groningen, Nijenborgh 16, 9747 AG Groningen, The Netherlands

Received January 30, 1992; Revised Manuscript Received July 7, 1992

ABSTRACT: Conformational studies were performed on a synthetic pentacosapeptide representing the RNA-binding N-terminal region of the coat protein of cowpea chlorotic mottle virus. Two-dimensional proton NMR experiments were performed on the highly positively charged peptide containing six arginines and three lysines in the presence of an excess of monophosphates, tetra(poly)phosphates, or octadeca(poly)-phosphates mimicking the phosphates of the RNA. The results show that the peptide alternates between various extended and helical structures in the presence of monophosphate and that this equilibrium shifts toward the helical structures (with the helical region situated between residues 10 and 20) in the presence of oligophosphates. Distance geometry calculations using distance constraints derived from a NOESY spectrum of the peptide in the presence of tetra(poly)phosphate resulted in eight structures belonging to two structure families. The first family consists of five structures with an α-helixlike conformation in the middle of the peptide, and the second family consists of three structures with a more open conformation. The propensity to form an α-helical conformation in the N-terminal part of this viral coat protein upon binding of phosphate groups to the positively charged side chains is suggested to play an essential role in RNA binding.

Cowpea chlorotic mottle virus (CCMV)[1] is an icosahedral plant virus consisting of RNA and 180 identical coat proteins, each 189 residues long (Dasgupta & Kaesberg, 1982). The virus particle can easily be dissociated and reassembled in vitro by changing pH and ionic strength (Bancroft & Hiebert, 1967). However, after removal of the first 25 amino acids by tryptic digestion, the protein is not able to bind the RNA anymore (Vriend et al., 1981). This indicates that the N-terminal arm containing nine positively charged amino acids (six Arg and three Lys) plays an essential role in RNA binding. On the basis of NMR experiments and secondary structure predictions, Vriend et al. (1982, 1986) proposed a model for the assembly of CCMV coat protein and RNA. In this "snatch–pull" model, the N-terminal region of the coat protein has a random coil conformation before interaction with the RNA but attains an α-helical conformation (between residues 10 and 20) upon binding of the positively charged side chains with the negatively charged phosphates of the RNA. Chemical synthesis of the pentacosapeptide P25 containing the first 25 N-terminal amino acids of CCMV coat protein (Ten Kortenaar et al., 1986) allowed detailed conformational studies to test the snatch–pull model. Circular dichroism experiments (Van der Graaf & Hemminga, 1991) showed that P25 has 15–18% α-helical conformation and about 80% random-coil conformation in the absence of salt at 25 °C and 20–21% α-helical conformation under the same conditions at 10 °C. Addition of inorganic salts results in an increase of α-helix content, up to 42% in the presence of octadeca(poly)phosphate. A two-dimensional proton NMR study on P25 in 200 mM sodium monophosphate, pH 4, showed that under these conditions P25 alternates between various extended and helical structures with the helical region situated between residues 9 and 17 (Van der Graaf et al., 1991). The objective of the present study is to determine the conformation of P25 in the presence of oligophosphates by two-dimensional proton NMR and distance geometry calculations in order to obtain more information about the conformational change of the N-terminal region of CCMV coat protein upon RNA binding.

MATERIALS AND METHODS

NMR Experiments. NMR samples contained 6.9–7.7 mM of the synthetic $N^{\alpha 1}$-acetyl-$C^{\alpha 25}$-methylamide (P25) [primary structure: STVGTGKLTRAQRRAAARKNKRNTR] (Ten Kortenaar et al., 1986) and 200 mM sodium monophosphate (P), 20 mM hexaammonium tetraphosphate (P_4), or 10 mM sodium octadecaphosphate (P_{18}) (sodium phosphate glass no. 15 of Sigma) in 10% (v/v) ^2H_2O and 90% (v/v) H_2O. The pH was 4 (for P) or 5 (for P_4 and P_{18}). All samples contained an excess of negatively charged (oligo)phosphates with respect to the amount of positively charged peptide present. Sodium 3-trimethylsilyl(2,2,3,3-$^2H_4$)propionate was used as an internal standard.

* Author to whom correspondence should be addressed.
‡ Agricultural University.
§ Present address: Department of Biochemistry, Gorlaeus Laboratories, University of Leiden, Einsteinweg 5, 2333 CC Leiden, The Netherlands.
∥ University of Groningen.
⊥ Present address: Department of Physical and Colloid Chemistry, Agricultural University, Dreijenplein 6, 6703 HB Wageningen, The Netherlands.

[1] Abbreviations: 2D, two dimensional; CCMV, cowpea chlorotic mottle virus; COSY, 2D scalar correlated spectroscopy; DG, distance geometry; δ_{conf}, conformation-dependent chemical shift; HOHAHA, 2D homonuclear Hartmann–Hahn transfer experiment; NMR, nuclear magnetic resonance; NOE, nuclear Overhauser enhancement; NOESY, 2D nuclear Overhauser enhancement spectroscopy; P, monophosphate; P_4, tetra(poly)phosphate; P_{18}, octadeca(poly)phosphate; P25, pentacosapeptide representing the N-terminus of the coat protein of CCMV; ppm, parts per million; rmsd; root mean square difference; RNA, ribonucleic acid.

0006-2960/92/0431-9177$03.00/0

Two-dimensional proton NMR spectra were recorded at 2, 5, and 10 °C on a Bruker AM 600 spectrometer interfaced with an Aspect 3000 computer. Phase-sensitive double-quantum-filtered COSY (Marion & Wüthrich, 1983; Rance et al., 1983), NOESY (Bodenhausen et al., 1984), and HOHAHA (Bax & Davis, 1985) spectra were obtained by using time-proportional phase incrementation in t_1. The carrier frequency was chosen in the middle of the spectrum coinciding with the water resonance. The water signal was suppressed by irradiation at all times except during data acquisition in COSY and NOESY experiments or only during the 2.5-ms relaxation delay in HOHAHA experiments. Further details concerning the 2D-NMR experiments on P25 in 200 mM sodium monophosphate have been described elsewhere (Van der Graaf et al., 1991). NOESY spectra of P25 in the presence of oligophosphates were recorded with mixing times of 100 and 200 ms for P25 + P_4 and 80 ms for P25 + P_{18}. No zero quantum suppression technique was applied. HOHAHA spectra were recorded with an MLEV-17 composite pulse of 75 ms for P25 + P_4 and 17 ms for P25 + P_{18}, preceded and followed by two 2.5-ms trim pulses. Since for P_{18} several resonances are broadened, the mixing time in the NOESY experiment and the MLEV-17 composite pulse in the HOHAHA experiment were chosen shorter for P_{18} than for P_4. Spectra were generally recorded with 512 t_1 increments of 2048 or 4096 data points. The number of scans per t_1 increment varied between 16 and 48 after 2 or 4 dummy scans. Data processing was performed as previously described (Van der Graaf et al., 1991).

Distance Geometry Calculations. Interproton distance constraints were derived from the NOESY spectrum of P25 in 20 mM P_4 recorded at 5 °C with a mixing time of 100 ms. NOE intensities were determined by counting contour levels in the NOESY contour plot. Intensities of peaks originating from overlapping methylene or methyl proton resonances were divided by 2 and 3, respectively. Interproton distances r_{ij} were calculated using

$$r_{ij} = (\mathrm{NOE}_{\mathrm{ref}}/\mathrm{NOE}_{\mathrm{obs}})^{1/6} r_{\mathrm{ref}}$$

where r_{ij} is the distance between protons i and j, r_{ref} is the reference distance, $\mathrm{NOE}_{\mathrm{obs}}$ is the observed NOE intensity, and $\mathrm{NOE}_{\mathrm{ref}}$ is the NOE intensity corresponding to the reference distance. The spectrum of P25 showed no NOESY cross peak between methylene proton resonances which was suitable for being used as a reference peak. Therefore, the NOESY cross peaks between the side-chain amide proton resonances of Gln and Asn, all showing equal intensities, were used as reference peaks (r_{ref} = 1.73 Å). To obtain the upper and lower limit of each interproton distance for the distance geometry calculations, a value of 0.5 Å was added to and subtracted from each r_{ij}. Additional pseudoatom corrections (Wüthrich et al., 1983) were applied in the case of degenerate methylene or methyl resonances (1.0 Å) and isopropyl groups (2.4 Å). Distances obtained for nondegenerate proton resonances (e.g., methylene protons) were not corrected, and the corresponding protons were labeled H1 (low-field resonance) and H2 (high-field resonance). In this way, 98 interresidual distance constraints were obtained from the NOESY spectrum of P25 (Appendix A in supplementary material). In addition, many other upper and lower bounds on distances in the peptide followed directly from the known bond lengths, bond angles, and atomic radii (holonomic constraints).

Distance geometry calculations were carried out on a Convex C1-XP computer using a program (written by R. M. Scheek) based upon the metric matrix method developed by Havel, Crippen, and Kuntz (Crippen, 1981; Crippen & Havel, 1978; Havel et al., 1983). By repeated random choices of interatomic distances between the upper and lower bounds, 48 different structures were generated. Each structure was optimized by minimizing the error function F_{error} by a 50-step conjugent gradient:

$$F_{\mathrm{error}} = K_{\mathrm{dc}}\{\sum_{d>u}(d^2 - u^2)^2 + \sum_{d<l}(d^2 - l^2)^2\} + K_{\mathrm{chiral}}\{\sum_{c}(v_c - V_c)^2\}$$

where K_{dc} is the force constant for the distance constraints (1 kJ·mol^{-1}·Å^{-4}), K_{chiral} is the force constant for the constraints on the chiral centers (1 kJ·mol^{-1}·Å^{-6}), d is an interproton distance in the generated structure, u is the upper limit distance constraint, l is the lower limit distance constrait, C is a chiral center, v_c is the signed volume of the chiral center in the generated structure, and V_c is the ideal signed volume of the chiral center. The chiral centers involving protons labeled H1 and H2 were not included in the error function, resulting in a "floating chirality" (Weber et al., 1988). The next step was a simplified molecular dynamics step to sample more exhaustively the possible conformations that satisfy the NMR distance constraints: 1000 steps (2 ps) of distance bounds driven dynamics (Kaptein et al., 1988) were performed at 1000 K, followed by a 1000-step cooling down to 1 K. During this "shaking up" of the structures the protons labeled H1 and H2 were flipped in a way comparable to the procedure Williamson and Madison (1990) used. Each tenth step H1 and H2 were interchanged, and the error functions corresponding to the situation before and after flipping (F_1 and F_2, respectively) were calculated. For $F_2 < F_1$ the structure generated by flipping was always chosen, but for $F_2 > F_1$ the structure generated was only chosen if

$$e^{-\Delta F/RT} > \epsilon$$

where $\Delta F = F_2 - F_1$, R is the gas constant (8.31 J·mol^{-1}·K), T is temperature, and ϵ is a value randomly chosen between 0 and 1. After this procedure the 32 structures showing the lowest values of F_{error} were selected. For interproton distances smaller than 4 Å present in those structures the NOESY spectrum was searched for corresponding cross peaks. In the case that certainly no NOESY cross peak was present, the distance was given a lower limit of 4 Å and an upper limit of 999.9 Å. In this way 36 non-NOE distance constraints were obtained (Appendix B in supplementary material). For the 32 structures generated before, these 36 non-NOE distance constraints were also included during a new run of 300 steps of distance bounds driven dynamics at 1000 K, followed by a 1000-step cooling down to 1 K. Finally, the eight structures showing the lowest values of F_{error} were selected. The NOE violations generally did not exceed 0.15 Å. The largest NOE violation (0.315 Å) was observed for the distance between αH of Thr9 and NH of Arg10 in structure 8. The violations of the homonomic constraints generally did not exceed 0.10 Å. The largest violation having a rather high value of 0.261 Å was observed for the distance between βC and βH2 of Gln12 in structure 3. The conformations of the eight structures were analyzed on an IRIS-4D/85GT work station of Silicon Graphics using the QUANTA 3.0/CHARMm software package of Polygen Corporation.

RESULTS

NMR Experiments. Figure 1 shows short- and medium-range NOESY connectivities present in the NOESY spectra

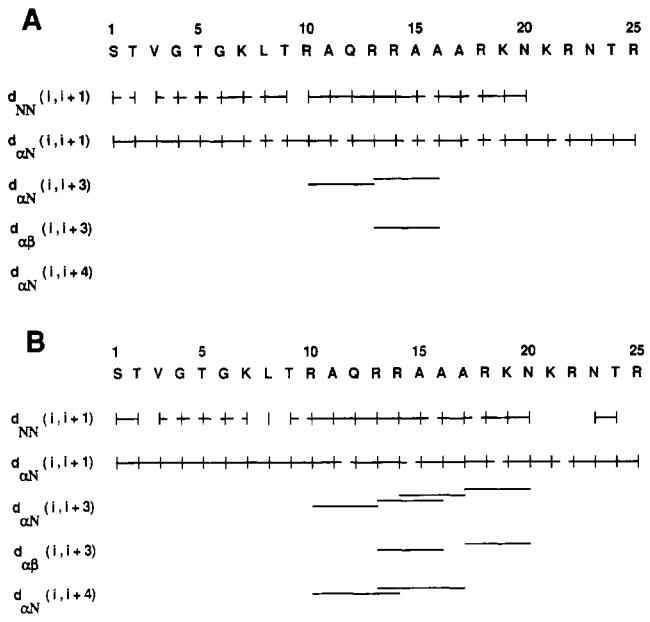

FIGURE 1: Summary of short- and medium-range NOEs observed at 10 °C for P25 in 200 mM sodium monophosphate, pH 4 (A), and for P25 in 20 mM hexaammonium tetraphosphate, pH 5 (B). Dashed lines indicate that the presence of the NOESY cross peak is ambiguous due to overlap with neighboring peaks.

of P25 in 200 mM sodium monophosphate, pH 4 (Figure 1A), and P25 in 20 mM hexaammonium tetraphosphate, pH 5 (Figure 1B), both recorded at 10 °C. Comparison of the spectrum of P25 in sodium monophosphate, pH 4, with the one-dimensional proton NMR spectrum of P25 in sodium monophosphate, pH 5, recorded at the same temperature (Van der Graaf & Hemminga, 1991) shows that the influence of the pH difference on the conformation of P25 is negligible. Details about the resonance assignment and determination of the conformation of P25 in 200 mM sodium monophosphate were described previously (Van der Graaf et al., 1991). The resonances in the spectrum of P25 in 20 mM hexaammonium tetraphosphate, pH 5, could easily be assigned with the help of the resonance assignment of P25 in 200 mM sodium monophosphate. The medium-range NOESY connectivities shown in Figure 1 [$d_{\alpha N}(i, i+3)$, $d_{\alpha\beta}(i, i+3)$, and $d_{\alpha N}(i, i+4)$] are characteristic of α-helical conformation (Wüthrich, 1986). Figure 2 shows a part of the NOESY spectrum of P25 in 20 mM hexaammonium tetraphosphate with the characteristic $d_{\alpha N}(i, i+3)$ and $d_{\alpha N}(i, i+4)$ connectivities indicated. Unfortunately it was not possible to analyze the NOESY spectrum of P25 in 10 mM sodium octadecaphosphate in the way as presented in Figure 1. In this spectrum only the resonances corresponding to the first six and last three residues of P25 were sharp and all other resonances were broadened. Probably the peptide can bind in different mutual exchanging conformations, which results in broadening of the resonances corresponding to the part of the peptide involved in phosphate binding. Medium-range NOESY connectivities could not be assigned, but it was possible to determine the chemical shifts of the α-protons. Figure 3 shows the conformation-dependent chemical shifts of the α-protons of P25 in the presence of monophosphate, tetraphosphate, and octadecaphosphate. These conformation-dependent chemical shifts were obtained by subtraction of the corresponding "random coil" chemical shifts (Bundi & Wüthrich, 1979) from the observed shifts.

Distance Constraints. Since the NOESY connectivities shown in Figure 1 indicate that P25 has a more stable structure in 20 mM hexaammonium tetraphosphate than in 200 mM

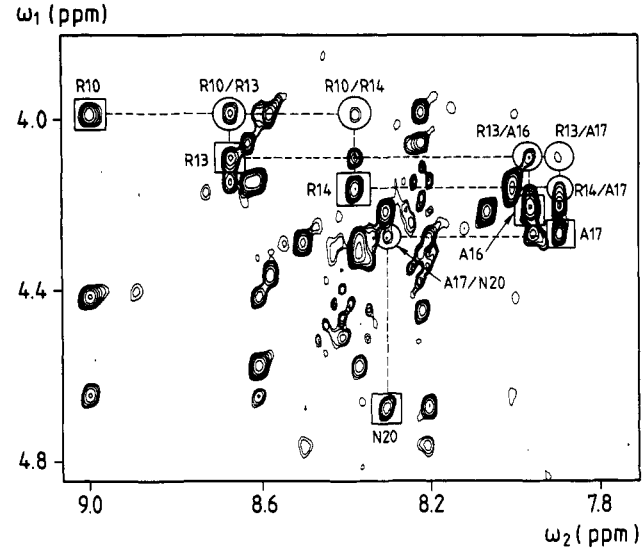

FIGURE 2: Part of a NOESY spectrum of 6.9 mM P25 in 20 mM hexaammonium tetraphosphate, pH 5, recorded with a mixing time of 100 ms at 10 °C. The time domain data consisting of 512 free induction decays of 2048 data points were multiplied by a sine-bell window function shifted by $\pi/6$ in both dimensions. The digital resolution in the transformed spectrum is 3.13 Hz/point in the ω_2 dimension and 6.26 Hz/point in the ω_1 dimension. Characteristic interresidual $d_{\alpha N}(i, i+3)$ and $d_{\alpha N}(i, i+4)$ connectivities are indicated by circles and labeled X_i/Y_{i+3} or X_i/Y_{i+4}. The corresponding intraresidual NH_i–αH_i connectivities are indicated by squares and labeled X_i.

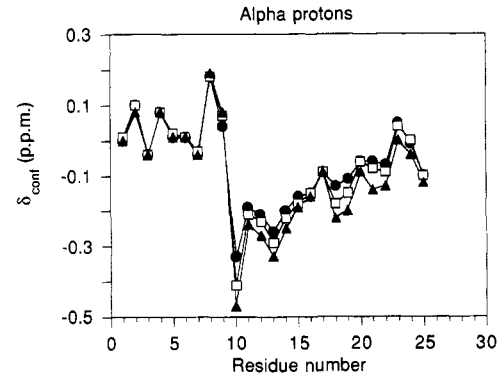

FIGURE 3: Conformation-dependent chemical shifts (δ_{conf}) of the α-protons of P25 in the presence of monophosphate (●), tetraphosphate (□), and octadecaphosphate (▲) measured at 10 °C. The conformation-dependent chemical shifts were obtained by subtraction of the corresponding "random coil" chemical shifts (Bundi & Wüthrich, 1979) from the measured chemical shifts.

sodium monophosphate, distance constraints for distance geometry calculations were derived from a NOESY spectrum of P25 in the presence of tetraphosphate. The NOESY spectrum recorded at 5 °C was used, because this spectrum showed less overlap than the NOESY spectrum recorded at 10 °C. Table I presents the complete resonance assignment of the proton NMR resonances of P25 in 20 mM hexaammonium tetraphosphate, pH 5, 5 °C. Interresidual NOE distance constraints and non-NOE distance constraints are presented in Appendixes A and B, respectively (see supplementary material).

Distance Geometry Structures. During the generation of the eight DG structures, some chiral centers had a "floating chirality". For each DG structure the chiral volumes of these centers were calculated to find out the positioning of the H1–H2 pairs. It turned out to be possible to assign the β-methylene protons of Arg14 stereospecifically, because the corresponding chiral volume showed a negative value in all

Table I: ^{1}H Chemical Shifts of 6.9 mM P25 in 20 mM Hexaammonium Tetraphosphate, pH 5.0, 5 °C

residue	chemical shift (ppm) NH	αH	βH	others
(Ac)				Ac-CH_3, 2.08
Ser1	8.50	4.50	3.90, 3.85	
Thr2	8.46	4.44	4.30	γCH_3, 1.22
Val3	8.27	4.13	2.10	γCH_3, 0.97, 0.97
Gly4	8.68	4.05		
Thr5	8.27	4.36	4.30	γCH_3, 1.23
Gly6	8.62	3.97		
Lys7	8.27	4.31	1.82, 1.75	γCH_2, 1.44, 1.41; δCH_2, 1.68, 1.68; εCH_2, 2.99, 2.99; ζNH_3^+, 7.66[a]
Leu8	8.42	4.58	1.68, 1.58	γCH, 1.70; δCH_3, 0.88, 0.83
Thr9	8.68	4.41	4.67	γCH_3, 1.33
Arg10	9.09	3.96	1.99, 1.88	γCH_2, 1.78, 1.62; δCH_2, 3.26, 3.26; εNH, 7.53
Ala11	8.67	4.13	1.45	
Gln12	8.03	4.13	2.37, 2.02	γCH_2, 2.46, 2.46; δNH_2, 7.63, 6.88
Arg13	8.74	4.07	1.96, 1.92	γCH_2, 1.81, 1.61; δCH_2, 3.27, 3.19; εNH, 7.25
Arg14	8.42	4.15	1.91, 1.91	γCH_2, 1.82, 1.71; δCH_2, 3.21, 3.21; εNH, 7.45
Ala15	8.03	4.16	1.49	
Ala16	7.99	4.20	1.47	
Ala17	7.92	4.26	1.50	
Arg18	7.98	4.20	1.92, 1.89	γCH_2, 1.79, 1.68; δCH_2, 3.23, 3.23; εNH, 7.41
Lys19	8.07	4.20	1.90, 1.86	γCH_2, 1.52, 1.46; δCH_2, 1.70, 1.70; εCH_2, 3.00, 3.00; ζNH_3^+, 7.66[a]
Asn20	8.32	4.68	2.89, 2.81	γNH_2, 7.75, 7.05
Lys21	8.22	4.26	1.91, 1.84	γCH_2, 1.51, 1.46; δCH_2, 1.71, 1.71; εCH_2, 3.01, 3.01; ζNH_3^+, 7.66[a]
Arg22	8.39	4.27	1.88, 1.84	γCH_2, 1.70, 1.63; δCH_2, 3.22, 3.22; εNH, 7.34
Asn23	8.52	4.78	2.92, 2.84	γNH_2, 7.78, 7.02
Thr24	8.25	4.33	4.28	γCH_3, 1.22
Arg25	8.39	4.27	1.87, 1.79	γCH_2, 1.67, 1.61; δCH_2, 3.21, 3.21; εNH, 7.30
($NHCH_3$)	7.97			CH_3, 2.75

[a] The Lys ζNH_3^+ resonance is broadened around 7.66 ppm due to exchange.

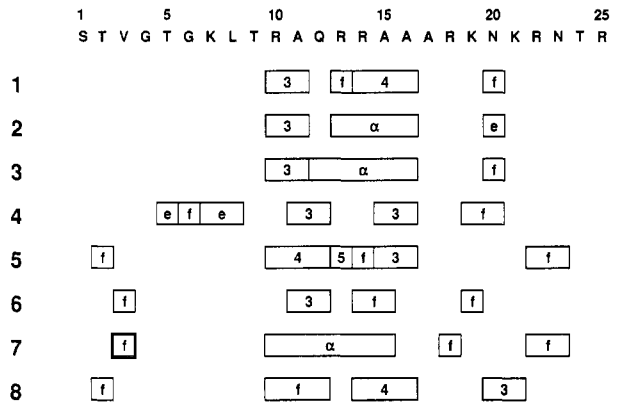

FIGURE 4: Secondary structure elements present in the DG structures 1–8 as determined according to Kabsch and Sander (1983). Definitions used: e = extended, CA torsion between −180° and −130°, or CA torsion between −130° and −100°, $\phi < -100°$, and $\psi > 100°$; f = folded, two or more consecutive residues with CA torsions between 30° and 70°; 3 = 3-turn: residues $i + 1$ and $i + 2$ are 3-turn if there exists H-bond (i, $i + 3$); 4 = 4-turn, residues $i + 1$, $i + 2$, and $i + 3$ are 4-turn if there exists H-bond (i, $i + 4$); 5 = 5-turn, residues $i + 1$, $i + 2$, $i + 3$, and $i + 4$ are 5-turn if there exists H-bond (i, $i + 5$); α = α-helix, two or more consecutive 4-turns.

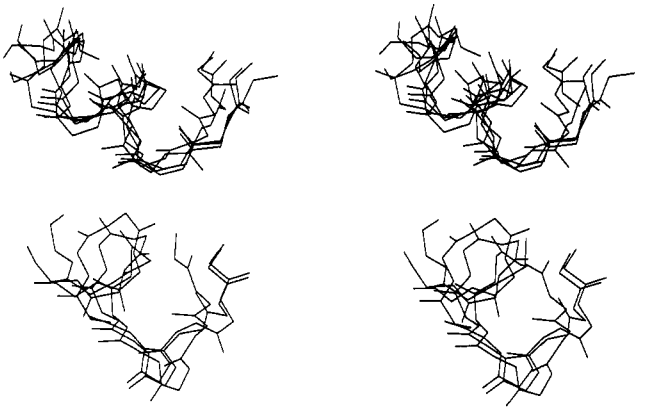

FIGURE 5: (top) Stereoview of a superposition of the backbone structures between residues 17 and 8 (from left to right) of the DG structures 1, 2, 3, 7, and 8. (bottom) Stereoview of a superposition of the backbone structures between residues 17 and 8 (from left to right) of the DG structures 4, 5, and 6.

eight structures. No further stereospecific assignments could be made. It should be noted that the procedure used only results in stereospecific assignments for protons which are situated in a region well-defined by NOE constraints, which is the case for the β-methylene protons of Arg14.

The conformation of each DG structure was analyzed according to the secondary structure determination procedure (Kabsch & Sander, 1983) present in the QUANTA/CHARMm software package. The results of this analysis (see Figure 4) shows that the region between residues 10 and 16 has a helical character in all DG structures. After the eight structures had been superimposed on each other, thereby optimizing the fit of the backbone atoms of residues 8–17, the root mean square deviations of the positions of these backbone atoms were calculated for all structure pairs to compare the backbone conformation in this region (see Table II). Table II shows that the eight DG structures can be divided into two structure families: family 1, consisting of structures 1, 2, 3, 7, and 8 (Figure 5, top) with an α-helixlike conformation, and family 2, consisting of structures 4, 5, and 6 (Figure 5, bottom) with a more open conformation. The structure families were chosen in a such way that within the two families each rmsd value corresponding to a structure pair is smaller than the average rmsd value of 2.328 Å.

Various DG structures were used as starting structures for molecular dynamics simulations in water using the CHARMm program to test the stability of the generated structures. Preliminary results show that structures with an open conformation in the middle of the peptide become α-helical and the other way round. Since no NOE restraints were applied during the simulations, it can be concluded that the

Table II: Root Mean Square Deviations[a] of the Backbone Atom Positions in the Region between Residues 8 and 17 for All Structure Pairs of the Eight DG Structures

	structure							
structure	1	2	3	7	8	4	5	6
1	0.000	1.136	1.221	0.779	1.064	3.174	2.962	3.156
2	1.136	0.000	0.964	0.813	1.857	3.594	3.154	3.405
3	1.221	0.964	0.000	1.181	1.597	3.190	3.439	3.276
7	0.779	0.813	1.181	0.000	1.475	3.313	2.998	3.240
8	1.064	1.857	1.597	1.475	0.000	2.836	3.219	3.166
4	3.174	3.594	3.190	3.313	2.836	0.000	2.324	1.140
5	2.962	3.154	3.439	2.998	3.219	2.324	0.000	1.501
6	3.156	3.405	3.276	3.240	3.166	1.140	1.501	0.000

[a] Root mean square deviations are given in angstroms. Average rmsd = 2.328 Å.

region in the middle of the peptide shows a natural tendency to become α-helical.

DISCUSSION

In the study presented here the conformation of P25 in the presence of P, P_4, and P_{18} was determined by two-dimensional proton NMR. In addition, NOE distance constraints obtained from the NOESY spectrum of P25 in the presence of P_4 were used to generate DG structures. Figure 1 shows medium-range NOESY connectivities characteristic of α-helical conformation present in NOESY spectra of P25 in 200 mM P (Figure 1A) and of P25 in 20 mM P4 (Figure 1B). This figure shows that in the presence of P_4 the number of these characteristic NOEs and the region where they appear increase. It can be concluded that the α-helical conformation in P25 is stabilized by the presence of P_4 and that the helical region is extended into the direction of the C-terminus. For exactly the same region as where the characteristic NOEs appear (between residues 10 and 20), Vriend predicted α-helix formation upon neutralization of the positive charges in the Arg and Lys side chains (Vriend et al., 1986). The δ_{conf} values presented in Figure 3 provide additional information about the backbone conformation of P25 in the presence of P, P_4, or P_{18}. Negative δ_{conf} values of the α-proton resonances are indicative of an α-helical conformation (Szilágyi & Jardetzky, 1989; Wagner et al., 1983). The negative values between residues 10 and 20 suggest that in this region (particularly close to residue 10) an α-helical conformation is favored, in agreement with the observed medium-range NOEs shown in Figure 1. Furthermore, it can be seen that the presence of oligophosphates of increasing length makes the δ_{conf} values of the α-proton resonances of P25 more negative, indicating a more stable helical conformation.

A previous 2D-NMR study on P25 in 200 mM sodium phosphate has shown that under the conditions used P25 alternates among extended and more helical structures on the NMR time scale (Van der Graaf et al., 1991). Since all NMR parameters including the NOE intensities are a population-weighted average over all conformations sampled, it is generally not possible to generate distance geometry structures for such systems not violating the distance constraints based upon the NOESY spectrum. Indeed, an attempt to generate DG structures by using distance constraints derived from a NOESY spectrum of P25 in 200 mM sodium monophosphate gave no satisfying results. A possible solution for this problem could be the use of an ensemble averaging [comparable with time averaging (Torda et al., 1989, 1990)] during the minimization of the error function in the distance geometry calculation, generating an ensemble of structures simultaneously. However, since the NMR data indicated that the helical conformation of P25 in the presence of P_4 was stabilized, the distance constraints derived from a NOESY spectrum of P25 and P_4 were used and the error function of each structure was optimized in the normal way. The NMR results can be accounted for in a regular α-helical conformation of P25 in the presence of P_4 (family 1; Figure 5, top). However, the data are also compatible with a somewhat distorted helical conformation (family 2; Figure 5, bottom). So on purely geometric arguments we cannot discriminate between these two or even conclude that both must be present in a conformational equilibrium. A more sophisticated modeling procedure of P25 and P_4 in solution, including a proper potential energy term and time- or ensemble-averaged restraints, will be needed to settle this point. Our present view, based on all NMR data and on preliminary molecular dynamics calculations, is that P25 fluctuates between regular α-helical and more open conformations in the presence of P_4, with P_4 favoring the α-helical conformations by electrostatic interactions.

On the basis of recent studies on P25 (Van der Graaf & Hemminga, 1991; Van der Graaf et al., 1991) in combination with the present results, it seems to be possible to extend the snatch–pull model (Vriend et al., 1982, 1986) to a more detailed model for the assembly of CCMV coat protein and RNA. It has been suggested before (Van der Graaf & Hemminga, 1991) that hydrogen-bond formation between the side chains of Thr9 and Gln12 may intiate α-helix formation in P25. After the formation of the first helical turn, the positive charge of Arg10 in combination with the induced positive charge of the helix dipole will attract negatively charged phosphate groups present in the RNA. Binding of a phosphate group to the side chain of Arg10 removes an unfavorable interaction between the positive charge in this side chain and the macrodipole of the helix, which may lead to an extension of the helix in the direction of the C-terminus (Hol, 1985; Shoemaker et al., 1985, 1987). The extension of the helical region results in the proper orientation of the other positively charged side chains for binding to the phosphate groups of the RNA backbone. In an α-helical conformation the distance between the arginines at positions 10, 14 and 18, and 22 ($\sim$6 Å) is comparable to the distance between two neighboring phosphate groups in an A-type RNA helix ($\sim$5.9 Å). In this way, the RNA may induce the conformation of the protein necessary for binding.

ACKNOWLEDGMENT

We thank Dr. D. Hartmann and S. Keim for performing molecular dynamics simulations. All NMR experiments were carried out at the SON HF-NMR facility in Nijmegen (The Netherlands).

SUPPLEMENTARY MATERIAL AVAILABLE

Appendix A, a table of NOE constraints used for DG calculations, and Appendix B, a table of non-NOE constraints used for DG calculations (5 pages). Ordering information is given on any current masthead page.

REFERENCES

Bancroft, J. B., & Hiebert, E. (1967) *Virology 32*, 354–356.
Bax, A., & Davis, D. G. (1985) *J. Magn. Reson. 65*, 355–360.
Bodenhausen, G., Kogler, H., & Ernst, R. R. (1984) *J. Magn. Reson. 58*, 370–388.
Bundi, A., & Wüthrich, K. (1979) *Biopolymers 18*, 285–297.
Crippen, G. M. (1981) *Distance Geometry and Conformational Calculations*, Research Studies Press, New York.

Crippen, G. M., & Havel, T. F. (1978) *Acta Crystallogr. 34A*, 282–284.
Dasgupta, R., & Kaesberg, P. (1982) *Nucleic Acids Res. 10*, 703–713.
Havel, T. F., Kuntz, I. D., & Crippen, G. M. (1983) *Bull. Math. Biol. 45*, 665–720.
Hol, W. G. J. (1985) *Prog. Biophys. Mol. Biol. 45*, 149–195.
Kabsch, W., & Sander, C. (1983) *Biopolymers 22*, 2577–2637.
Kaptein, R., Boelens, R., Scheek, R. M., & Van Gunsteren, W. F. (1988) *Biochemistry 27*, 5389–5395.
Marion, D., & Wüthrich, K. (1983) *Biochem. Biophys. Res. Commun. 113*, 967–974.
Rance, M., Sørensen, O. W., Bodenhausen, G., Wagner, G., Ernst, R. R., & Wüthrich, K. (1983) *Biochem. Biophys. Res. Commun. 117*, 479–485.
Shoemaker, K. R., Kim, P. S., Brems, D. N., Marquesee, S., York, E. J. Chaiken, I. M., Stewart, J. M., & Baldwin, R. L. (1985) *Proc. Natl. Acad. Sci. U.S.A. 82*, 2349–2353.
Shoemaker, K. R., Kim, P. S., York, E. J., Stewart, J. M., & Baldwin, R. L. (1987) *Nature 326*, 563–567.
Szilágyi, L., & Jardetzky, O. (1989) *J. Magn. Reson. 83*, 441–449.
Ten Kortenaar, P. B. W., Krüse, J., Hemminga, M. A., & Tesser, G. I. (1986) *Int. J. Pept. Protein Res. 27*, 401–413.
Torda, A. E., Scheek, R. M., & Van Gunsteren, W. F. (1989) *Chem. Phys. Lett. 157*, 289–294.
Torda, A. E., Scheek, R. M., & Van Gunsteren, W. F. (1990) *J. Mol. Biol. 214*, 223–235.
Van der Graaf, M., & Hemminga, M. A. (1991) *Eur. J. Biochem. 201*, 489–494.
Van der Graaf, M., Van Mierlo, C. P. M., & Hemminga, M. A. (1991) *Biochemistry 30*, 5722–5727.
Vriend, G., Hemminga, M. A., Verduin, B. J. M., de Wit, J. L., & Schaafsma, T. J. (1981) *FEBS Lett. 134*, 167–171.
Vriend, G., Verduin, B. J. M., Hemminga, M. A., & Schaafsma, T. J. (1982) *FEBS Lett. 145*, 49–52.
Vriend, G., Verduin, B. J. M., & Hemminga, M. A. (1986) *J. Mol. Biol. 191*, 453–460.
Wagner, G., Pardi, A., & Wütherich, K. (1983) *J. Am. Chem. Soc. 105*, 5948–5949.
Weber, P. L., Morrison, R., & Hare, D. (1988) *J. Mol. Biol. 204*, 483–487.
Williamson, M. P., & Madison, V. S. (1990) *Biochemistry 29*, 2895–2905.
Wüthrich, K. (1986) *NMR of Proteins and Nucleic Acids*, Wiley, New York.
Wüthrich, K., Billeter, M., & Braun, W. (1983) *J. Mol. Biol. 169*, 949–961.

Registry No. P, 14265-44-2; P_4, 16132-64-2; P25, 105366-49-2; polyphosphate, 131095-82-4.